

ARTICLE

State-to-state Photoionization Dynamics of Vanadium Nitride by Two-color Laser Photoionization and Photoelectron Methods[†]Huang Huang^a, Zhi-hong Luo^a, Yih Chung Chang^a, Kai-Chung Lau^b, C. Y. Ng^{a*}*a.* Department of Chemistry, University of California, Davis, CA 95616, USA*b.* Department of Biology and Chemistry, City University of Hong Kong, Kowloon, Hong Kong, China

(Dated: Received on November 6, 2013; Accepted on November 29, 2013)

We have conducted a two-color visible-ultraviolet (VIS-UV) resonance-enhanced laser photoionization and pulsed field ionization-photoelectron (PFI-PE) study of gaseous vanadium mononitride (VN) in the total energy range of 56900–59020 cm⁻¹. The VN molecules were selectively excited to single rotational levels of the intermediate VN(*D*³Π₀, *v*'=0) state by using a VIS dye laser prior to photoionization by employing a UV laser. This two-color scheme allows the measurements of rovibronically selected and resolved PFI-PE spectra for the VN⁺(*X*²Δ; *v*⁺=0, 1, and 2) ion vibrational bands. By simulating the rotationally resolved PFI-PE spectra, *J*⁺=3/2 is determined to be the lowest rotational level of the ground electronic state, indicating that the symmetry of the ground VN⁺ electronic state is ²Δ_{3/2}. The analysis of the PFI-PE spectra for VN⁺ also yields accurate values for the adiabatic ionization energy for the formation of VN⁺(*X*²Δ_{3/2}), IE(VN)=56909.5±0.8 cm⁻¹ (7.05588±0.00010 eV), the vibrational frequency ω_e⁺=1068.0±0.8 cm⁻¹, the anharmonicity constant ω_e⁺χ_e⁺=5.8±0.8 cm⁻¹, the rotational constants *B*_e⁺=0.6563±0.0005 cm⁻¹ and α_e⁺=0.0069±0.0004 cm⁻¹, and the equilibrium bond length, *r*_e⁺=1.529 Å, for VN⁺(*X*²Δ_{3/2}); along with the rotational constants *B*_e⁺=0.6578±0.0028 cm⁻¹ and α_e⁺=0.0085±0.0028 cm⁻¹, and the equilibrium bond length *r*_e⁺=1.527 Å for VN⁺(*X*²Δ_{5/2}), and the spin-orbit coupling constant *A*=153.3±0.8 cm⁻¹ for VN⁺(*X*²Δ_{5/2,3/2}). The highly precise energetic and spectroscopic data obtained in the present study are valuable for benchmarking the predictions based on state-of-the-art *ab initio* quantum calculations.

Key words: Vanadium nitride, Vanadium nitride cation, Photoionization dynamics, Two-color photoionization, Pulsed field ionization-photoelectron, Ionization energy, Bond dissociation energy

I. INTRODUCTION

Detailed bonding properties of transition metal-containing molecules are important in many basic and applied research fields, including organometallic chemistry, catalysis, and astrophysics [1]. The accurate bonding descriptions between transition metal atoms (M's) and main group species are partly complicated by the involvement of d-shell electrons associated with transition metal atoms. The existence of unpaired d-shell electrons is known to give rise to many low lying excited electronic states with different multiplicities. As a result, extensive electron correlations are required in order to achieve accurate spectroscopic and energetic predictions of transition metal-containing

molecules and their ions by *ab initio* quantum chemical calculations [1]. In view of the lack of accurate energetic database for this class of compounds, we have recently initiated an experimental program based on high resolution photoionization efficiency (PIE), pulsed field ionization-photoelectron (PFI-PE), and photodissociation measurements, aiming to determine accurate spectroscopic data, such as rotational constants and vibrational frequencies, and energetic properties, such as ionization energies (IE's) and 0 K bond dissociation energies (*D*₀'s), of transition metal carbides, oxides, and nitrides (MX's) and their cations (MX⁺'s) (*X*=C, O, and N). The highly precise IE and *D*₀ values thus obtained have not only enhanced the spectroscopic and energetic database for these MX/MX⁺ systems, but also served as valuable benchmarks for comparison with predictions of state-of-the-art *ab initio* quantum chemical calculations. Being the simplest molecular systems, the rigorous experimental and theoretical comparisons are expected to provide fundamental insight into the M–X and M⁺–X bonding interactions.

[†]Part of the special issue for “the Chinese Chemical Society's 13th National Chemical Dynamics Symposium”.

*Author to whom correspondence should be addressed. E-mail: cyng@ucdavis.edu

Several experimental and theoretical studies of VN have been reported [2–6]. Peter *et al.* have recorded the (0, 0) band of the electronic emission system of VN at around 700 nm and identified the transitions as the $A^3\Phi-X^3\Delta$ transition system, yielding spectroscopic constants for both the upper and lower states [5]. A laser-induced fluorescence study on the $d^1\Sigma^+-X^3\Delta_1$ transition system of VN was reported by Simard *et al.* at about the same time [6]. Subsequently, Balfour *et al.* have performed a high resolution spectroscopic study of the $D^3\Pi-X^3\Delta$ transition system by using the laser ablation and laser-induced fluorescence techniques [2]. Despite these high-resolution study of the neutral VN states, no spectroscopic investigation on cationic VN^+ states has been reported besides a very crude IE(VN) estimate of 8 ± 1 eV [7]. On the theoretical side, the electronic structures of neutral VN in its ground and low-lying excited states have been investigated by Harrison at the *ab initio* MCSCF and multireference configuration levels of theory [3]. Kunze *et al.* have also explored the electronic structures of cationic VN^+ by employing similar theoretical methods [4].

Recently, we have successfully investigated the FeC^+ , NiC^+ , CoC^+ and TiO^+ cations by means of two-color visible (VIS)-ultraviolet (UV) resonance-enhanced PIE and PFI-PE measurements [8–11]. By first selectively exciting MC (MO) to a single rovibronic level of an intermediate neutral state MX^* by using a VIS dye laser prior to photoionization by a UV dye laser, we have been able to significantly enhance the PIE and PFI-PE signals for MX^+ and at the same time reduced the interference from transition metal atoms and other clusters, which are also produced in the laser ablation supersonic beam source. The VIS-UV PFI-PE spectra for FeC^+ , NiC^+ , CoC^+ , and TiO^+ thus obtained are found to be rotationally well resolved, making possible the unambiguous rotational assignments of the PFI-PE spectra. The highly precise IE(MC) (IE(MO)) and $D_0(M^+-C)-D_0(M-C)$ [$D_0(M^+-O)-D_0(M-O)$] values determined in the PFI-PE experiments have been used to benchmark the state-of-the-art *ab initio* quantum chemical calculations. While the experimental energetic values were found to deviate significantly from the theoretical predictions obtained by using the multireference variation method at the C-MRCI+Q level of theory and density functional theory (DFT) calculations for the FeC/FeC^+ , NiC/NiC^+ and CoC/CoC^+ systems, the CCSDTQ/CBS approach, which involves the approximation to the complete basis set (CBS) limit at the coupled cluster level up to quadruple excitations, has been shown to provide reliable theoretical energetic predictions with deviations to be within ± 45 meV compared to experimental measurements [12–14].

In order to include similar theoretical and experimental comparisons for transition metal nitride species, we have extended our high-resolution VIS-UV PIE and PFI-PE measurements to the VN/VN^+ system. In this work, we report the spectroscopic and energetic

results for VN and VN^+ obtained from the analysis of the PIE and PFI-PE measurements. In addition to the results of previous studies on the FeC/FeC^+ , NiC/NiC^+ , CoC/CoC^+ , and TiO/TiO^+ systems, the present high-resolution PFI-PE study on the VN/VN^+ system is expected to provide further test of the *ab initio* CCSDTQ/CBS computation procedures for accurate energetic and structural predictions of transition metal-containing compounds.

II. EXPERIMENTS

The experimental apparatus and procedures used are essentially the same as those employed in the studies on the FeC/FeC^+ , NiC/NiC^+ , CoC/CoC^+ , and TiO/TiO^+ systems and have been described in detail previously [8–11]. Briefly, the apparatus consists of a Smalley-type laser ablation supersonic beam source for the generation of cold VN molecules, two dye lasers pumped by a Nd:YAG laser for two-color resonance-enhanced photoionization measurements, a time-of-flight (TOF) mass spectrometer for photoion detection, and a TOF spectrometer for PFI-PE detection. The two dye lasers used in this experiment are the Lambda Physik FL 3002 (VIS output= ω_1 , optical bandwidth= 0.2 cm^{-1} (full-width at half-maximum, FWHM)) and FL 2002 (UV output= ω_2 , optical bandwidth= 0.4 cm^{-1} (FWHM)) dye lasers, which were pumped by the same Nd:YAG laser (Spectra-Physics, Quanta-Ray Pro 230; repetition rate=30 Hz).

Gaseous VN molecules were produced by reacting V atoms with NH_3 (5% NH_3 seeded in He as the carrier gas). The V atoms were generated by laser ablation of a rotating and translating vanadium rod (American Element, 99% purity) by using the second harmonic (532 nm) output of a Nd:YAG laser (Continuum, Surelite-1-30) operating at 30 Hz with a pulse energy of ~ 2 mJ. The gaseous VN sample thus formed was cooled by supersonic expansion and skimmed by a circular skimmer (diameter=1 mm) in the beam source chamber prior to entering the photoionization/photoexcitation (PI/PEX) region in the photoionization chamber. A pair of deflection plates was installed between the skimmer and the PI/PEX region and a DC field of 150 V/cm was applied on the deflection plates to prevent the charged and metastable high- n Rydberg species produced in the laser ablation source from entering the PI/PEX region. This arrangement was found to be effective in reducing the background noise in PFI-PE measurements.

The ions formed by photoionization were extracted toward the TOF mass spectrometer for detection by the ion MCP detector by applying a DC electric field of 10 V/cm in the PI/PEX region. For PFI-PE measurements, it is necessary to keep the PI/PEX region field free during the laser excitation in order to minimize the destruction of high- n Rydberg species. Hence

a pulsing scheme similar to that used in CoC/CoC⁺ and TiO/TiO⁺ experiments was adopted [9, 11]. An electric field of 0.1 V/cm for the dispersion of prompt background electrons was applied to the PI/PEX region at a delay of 150 ns with respect to the application of the UV ω_2 laser pulse. The electric field pulse of 0.7 V/cm for PFI and the extraction of PFI-PEs toward the electron MCP detector was turned on at a delay of 1.5 μ s with respect to the UV ω_2 laser pulse. The energies of both dye lasers were calibrated by using a Coherent WaveMaster to a precision of ± 0.04 cm⁻¹.

The ion or electron signal from the MCP detector was amplified by a fast preamplifier (LeCroy research system, 612AM) before being fed into a gated boxcar integrator (Stanford Research system, SR250) for data integration. The analog signal thus obtained was converted to digital data by using an analog to digital converter (Stanford research system, SR245) for data processing by a personal computer. At each setting of the laser energies, the data obtained represent the average of 30 laser shots; and the photoion and PFI-PE intensities have been normalized by the UV ω_2 laser power. All PIE and PFI-PE spectra presented in this work are the average of at least four independent, reproducible scans.

III. RESULTS AND DISCUSSION

Similar to the previous studies, the first step of the experiment is to identify a rotationally resolved band corresponding to the transition to an intermediate state from the ground state of VN so that rovibrationally well resolved PFI-PE spectra can be obtained. Due to the spin-orbit coupling, the ground ³ Δ state of VN is split into three sublevels approximately 150 cm⁻¹ apart. Thus it is important to make the correct rotational assignments of the PFI-PE spectra. After surveying the transition bands in the visible region, the VN* ($D^3\Pi_0$, $v'=0$) vibronic band was picked as the intermediate state for the subsequent PIE and PFI-PE measurements. The upper spectrum in Fig.1 depicts the band corresponding to the formation of VN* ($D^3\Pi_0$, $v'=0$) from the VN ($X^3\Delta_1$, $v''=0$) ground state recorded by fixing the energy of UV ω_2 at 47619 cm⁻¹ and scanning the energy of the VIS ω_1 while measuring the intensity of VN⁺ signal. According to the standard formula, for the vibrational energy:

$$G(v) = \omega_e \left(v + \frac{1}{2} \right) - \omega_e \chi_e \left(v + \frac{1}{2} \right)^2 \quad (1)$$

and for the rotational energy:

$$F(J) = B[J(J+1) - \Omega^2] \quad (2)$$

the energy of the VN* ($D^3\Pi_0$, $v'=0$, J') \leftarrow VN($X^3\Delta_1$, $v''=0$, J'') transition can be written as

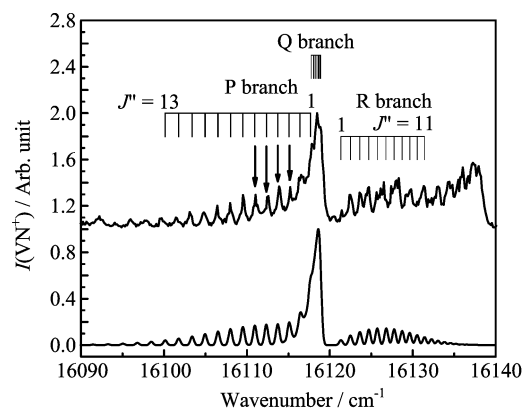


FIG. 1 The rotational-resolved excitation spectrum (upper spectrum) for the formation of the intermediate VN* ($D^3\Pi_0$, $v'=0$, J') rovibronic states from the VN ($X^3\Delta_1$, $v''=0$, J'') ground state. This spectrum was recorded by means of two-color VIS-UV laser resonance-enhanced photoionization scheme, in which the UV ω_2 laser was fixed at 47619 cm⁻¹ and the VIS ω_1 laser was scanned in the energy range of 16090–16140 cm⁻¹. The simulated spectrum (lower curve) was obtained by using a Gaussian instrumental line profile (FWHM=0.5 cm⁻¹) and a Boltzmann rotational temperature of 35 K for the VN molecular beam. The rotational assignments are marked on top of the experimental spectrum.

$$v = v_{00} + B'[J'(J'+1) - \Omega'^2] - B''[J''(J''+1) - \Omega''^2] \quad (3)$$

$$v_{00} = \Delta T_{e'e''} + \left(\frac{\omega_{e'}}{2} - \frac{\omega_{e'}\chi_{e'}}{4} \right) - \left(\frac{\omega_{e''}}{2} - \frac{\omega_{e''}\chi_{e''}}{4} \right) \quad (4)$$

where $\Delta T_{e'e''}$ is the energy difference between the potential minimum of the excited electronic state and that of the ground electronic state, $\omega_{e'}$ and $\omega_{e'}\chi_{e'}$ ($\omega_{e''}$ and $\omega_{e''}\chi_{e''}$) are the harmonic frequency and anharmonicity constant for the excited (ground) state, B' (B'') is the rotational constant for the excited (ground) state, J' (J'') is the total angular momentum for the excited (ground) state and Ω' (Ω'') is the total electronic angular momentum about the internuclear axis for the excited (ground) state. Balfour *et al.* have determined the rotational constant $B''=0.6253286$ cm⁻¹ for the VN ($X^3\Delta_1$, $v''=0$) ground state and $B'=0.6091451$ cm⁻¹ for the VN* ($D^3\Pi_0$, $v'=0$) state [2]. These values were adopted directly in the simulation process. According to Eq.(1), we have obtained the simulated spectrum (lower spectrum in Fig.1) by assuming a Gaussian instrumental profile (FWHM=0.5 cm⁻¹) and a Boltzmann distribution of the rotational levels for the VN($X^3\Delta_1$, $v''=0$) state governed by a rotational temperature of 35 K. The assignments of the transitions are labeled on top of the experimental spectrum. The observation that the lowest allowed value for J' is 0, confirming that the excited state is of ³ Π_0 symmetry and thus the initial state is consistent with the $X^3\Delta_1$ state. In order to obtain rotationally resolved PFI-PE spectra in the subsequent UV photoionization measure-

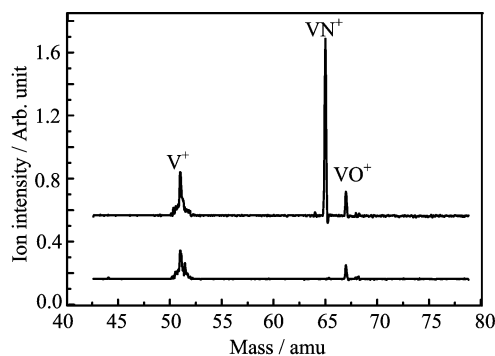


FIG. 2 The upper spectrum is the TOF mass spectrum for V^+ , VN^+ and VO^+ observed by means of two-color VIS-UV resonance enhanced photoionization scheme with VIS ω_1 fixed at 16113.88 cm^{-1} and UV ω_2 fixed at 47619 cm^{-1} . The lower spectrum was recorded by means of one-color UV multi-photon ionization scheme, *i.e.*, the VIS ω_1 laser beam was turned off and only the UV ω_2 laser was turned on.

ment, it is desirable to select individual transition lines which are well resolved and free of contamination from other transitions. The comparison of the experimental and simulated spectra in Fig.1 shows that the transition lines in the R-branch have irregular peak shapes and intensities, suggesting that of the R-branch is likely overlapping with other transitions. For this reason, we have selected rotational transitions of the P-branch, P(3), P(4), P(5), and P(6) (as marked by downward pointing arrows in Fig.1) for preparing $VN^*(D^3\Pi_0, v'=0)$ in single rotational levels, $J'=2$, $J'=3$, $J'=4$, or $J'=5$, respectively for subsequent UV photoionization.

The TOF spectrum recorded by means of two-color VIS-UV resonance-enhanced photoionization scheme with VIS ω_1 fixed at 16113.88 cm^{-1} , the energy of P(4) line, and UV ω_2 fixed at 47619 cm^{-1} is shown as the upper spectrum in Fig.2. While the lower spectrum was obtained when the VIS ω_1 laser beam was turned off, *i.e.*, only the UV ω_2 laser beam was employed to interact with the molecule beam. The peaks at 51, 65, and 67 amu are assigned as the ion peaks for V^+ , VN^+ and VO^+ respectively. The VO molecules in the molecular beam were probably produced from VO coating of the V rod. In this experiment, high purity (99.99%) He was used as the carrier gas. Based on the comparison between the upper and lower spectra in Fig.2, almost all VN^+ ions were shown to be produced by two-color VIS-UV laser resonance-enhanced photoionization because the VN^+ signal fell to the noise level when the VIS ω_1 laser was turned off. While nearly all V^+ and VO^+ ions were generated by single-color UV two-photon or multi-photon ionization, we found that the intensities of V^+ and VO^+ were not affected by the VIS ω_1 laser.

The PIE spectrum of VN depicted in Fig.3 has been measured by setting the VIS ω_1 fixed at 16113.88 cm^{-1} , the energy of P(4) line, and recording the intensity of VN^+ ion signal while scanning the UV ω_2 laser output

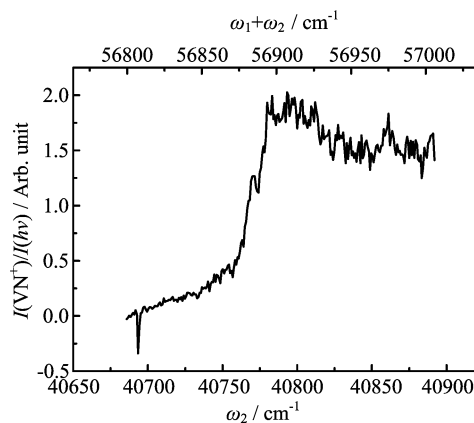


FIG. 3 The PIE spectrum for the formation of $VN^+(X^2\Delta, v^+=0)$ recorded by using the two-color VIS-UV laser resonance-enhanced photoionization scheme, in which the VIS ω_1 was fixed at $\omega_1=16113.88\text{ cm}^{-1}$, while the UV ω_2 was scanned in the energy range of $40700\text{--}40900\text{ cm}^{-1}$. The bottom energy scale represents the sum of the VIS and UV ($\omega_1+\omega_2$) energy. The step-like onset at 56885 cm^{-1} is identified to be corresponding to the formation of $VN^+(X^2\Delta, v^+=0)$ state.

in the energy range from 40700 cm^{-1} to 40900 cm^{-1} (bottom energy scale of Fig.3). The top energy scale of Fig.3 represents the total energy of the VIS and UV photons ($\omega_1+\omega_2$). The PIE of VN^+ represents the VN^+ ion intensity normalized by the intensity of UV ω_2 . The PIE onset at 56885 cm^{-1} can be identified as the IE(VN) for the formation of the ground state of VN^+ . The observation of the PIE onset is an important step for the PFI-PE measurements to be focused at the relevant photon energy range. As shown below, the IE(VN) value obtained by PFI-PE measurements is significantly more precise than that based on that marked by the PIE step.

The lower spectra in Fig.4 show the PFI-PE spectra for the formation of $VN^+(X^2\Delta_{3/2}, v^+=0, J^+)$ obtained by fixing the VIS ω_1 laser output at the respective excitation energies of the P(3), P(4), P(5), and P(6) lines and measuring the PFI-PE intensity while scanning the UV ω_2 laser output in the energy range from 40750 cm^{-1} to 40830 cm^{-1} . The top energy scale represents the total energy of the VIS and UV photons ($\omega_1+\omega_2$) in the energy region of $56870\text{--}56940\text{ cm}^{-1}$. Since we have been able to selectively excite VN molecules to $J'=2$, $J'=3$, $J'=4$, or $J'=5$ level of $VN^*(D^3\Pi_0, v'=0)$ state, the rotationally well resolved peaks observed in the PFI-PE spectra represent the transitions to single $VN^+(X^2\Delta_{3/2}, v^+=0, J^+)$ rovibronic states. On the basis of a standard formula similar to Eq.(1), we have successfully simulated the experimental VIS-UV PFI-PE spectra by assuming a Gaussian instrumental profile (FWHM= 1.8 cm^{-1}). The simulated spectra are shown as the upper spec-

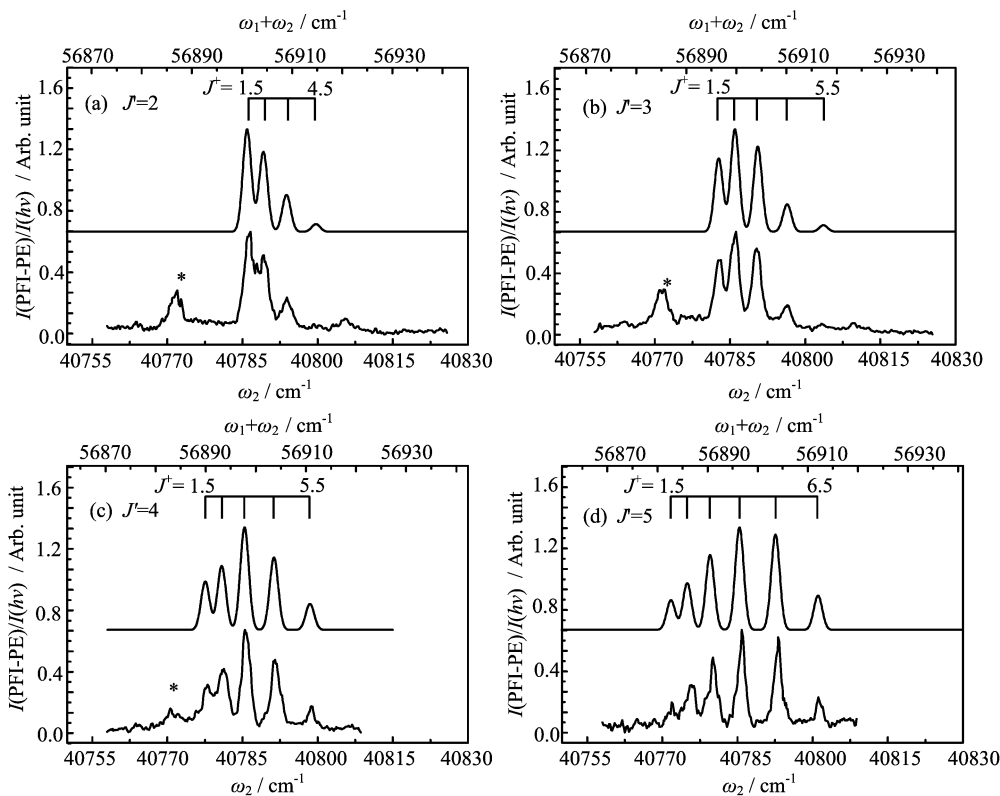


FIG. 4 Rotationally resolved PFI-PE spectra (lower spectra) in the total $\omega_1+\omega_2$ energy region of 56870–56940 cm^{-1} (top energy scale) for the formation of $\text{VN}^+(X^2\Delta_{3/2}, v^+=0, J^+)$ from the rotational levels, (a) $J'=2$, (b) $J'=3$, (c) $J'=4$, and (d) $J'=5$, of the intermediate $\text{VN}^*(D^3\Pi_0, v'=0)$ state. The corresponding UV ω_2 energies are in the range of 40750–40830 cm^{-1} (bottom energy scale). These J' levels were populated by setting the VIS ω_1 energy at the respective P(3), P(4), P(5), and P(6) transition lines shown in Fig.1. The simulated spectra obtained by assuming a Gaussian instrumental line profile (FWHM=1.8 cm^{-1}) for the PFI-PE energy resolution profile are shown as the upper spectra in (a)–(d).

tra in Fig.4, on top of which the J^+ -rotational assignments are labeled. The intensity of each peak in the simulated spectra was adjusted to fit the experimental spectra. It should be noted that some of the peaks (marked with asterisk) cannot be assigned, which could be attributed to impurity rotational states, which are different from the targeted $J'=2$, $J'=3$, $J'=4$, or $J'=5$ levels of $\text{VN}^*(D^3\Pi_0, v'=0)$ prepared in the VIS excitation. The simulation results show that the lowest allowed value of J^+ is 3/2, indicating that $\Omega^+=3/2$ and the ground electronic state of VN^+ is of $^2\Delta_{3/2}$ symmetry. By fitting the observed rotational transitions of the PFI-PE spectra, we have determined that the rotational constant $B_0^+=0.6530\pm 0.0020$ cm^{-1} and the band origin $\nu_{00}^+=56909.1\pm 0.8$ cm^{-1} for the formation of the $\text{VN}^+(X^2\Delta_{3/2}, v^+=0)$ ground state after taking into account the stark shift.

We found in our previous VIS-UV PFI-PE study of the TiO/TiO^+ system that the $^2\Delta$ ground state of TiO^+ is split into two sub-states due to the spin-orbit coupling interaction [9]. Since VN is isoelectronic to TiO , it is expected that the $^2\Delta$ ground state of VN^+ is also split into two sub-states. According to this expect-

ation, we observed the excited PFI-PE band for the $\text{VN}^+(X^2\Delta_{5/2}, v^+=0)$ spin-orbit state at ~ 300 cm^{-1} higher than the PFI-PE band for the $\text{VN}^+(X^2\Delta_{3/2}, v^+=0)$ ground state. The PFI-PE spectra for the formation of $\text{VN}^+(X^2\Delta_{5/2}, v^+=0, J^+)$ was obtained by measuring the PFI-PE intensity for VN^+ while fixing the VIS ω_1 laser output at the transition energy of the P(3), P(4), P(5) or P(6) lines and scanning the UV ω_2 laser output from 41060 cm^{-1} to 41130 cm^{-1} . The respective PFI-PE spectra thus obtained are plotted as the lower spectra in Fig.5. The top energy scale represents the total energy of the VIS and UV photons ($\omega_1+\omega_2$) in the energy region of 57175–57245 cm^{-1} . The dominant peaks marked with asterisks in the PFI-PE spectra are likely to originate from UV two-photon or multiphoton ionization of V or VO because the positions and intensities of these unassigned background peaks were found to depend solely on the UV ω_2 laser output. The upper spectra in Fig.5 are the corresponding simulated spectra obtained by assuming a Gaussian instrumental profile (FWHM=1.8 cm^{-1}). The well resolved experimental VIS-UV PFI-PE spectra allow unambiguous rotational assignments for the observed

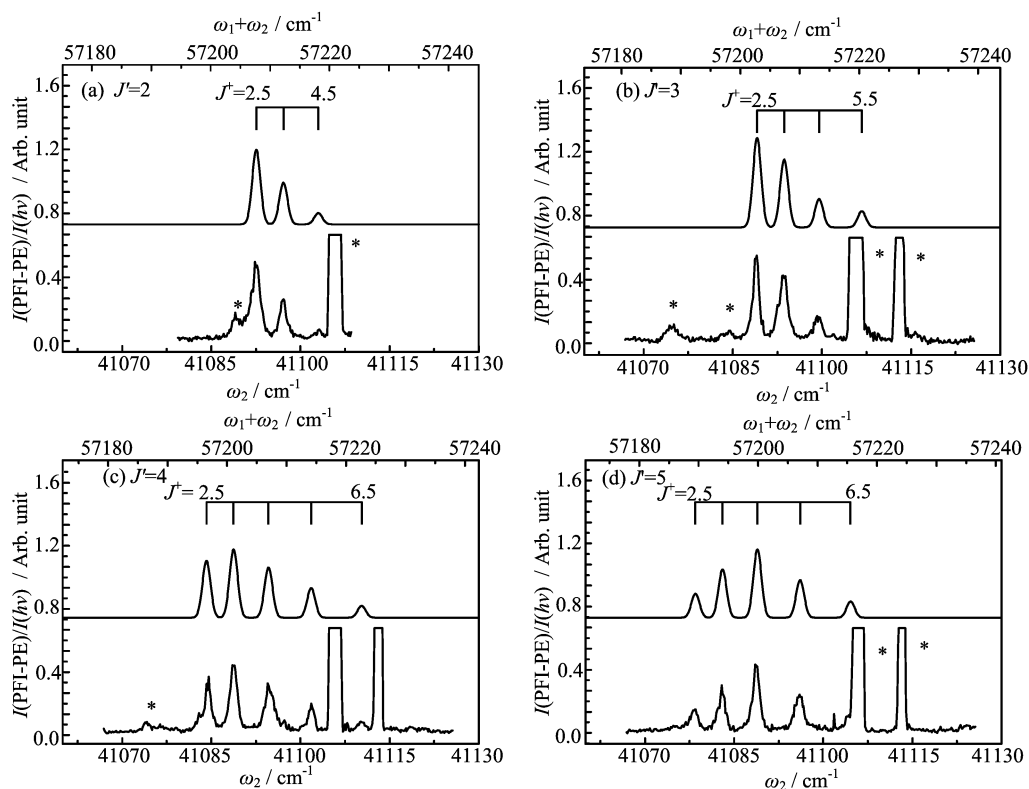


FIG. 5 Rotationally resolved PFI-PE spectra (lower) and the simulated spectra (upper) for the formation of $\text{VN}^+(X^2\Delta_{5/2}, v^+=0, J^+)$ from the rotational levels, (a) $J'=2$, (b) $J'=3$, (c) $J'=4$, and (d) $J'=5$, of the intermediate $\text{VN}^*(D^3\Pi_0, v'=0)$ state.

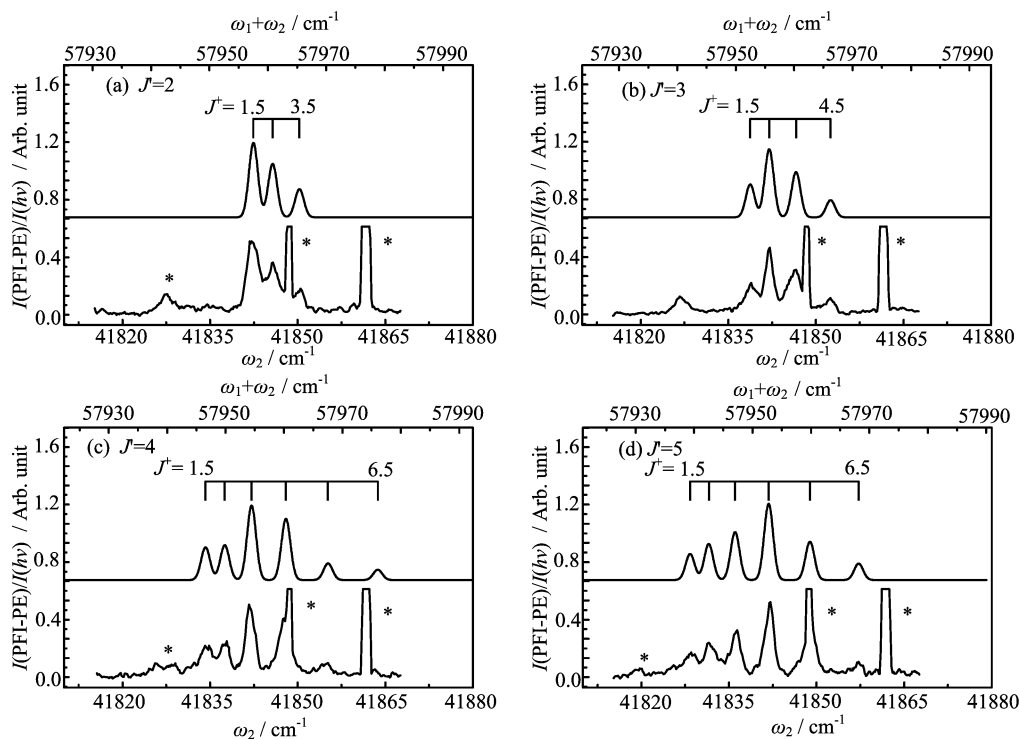


FIG. 6 Rotationally resolved PFI-PE spectra (lower) and the simulated spectra (upper) for the formation of $\text{VN}^+(X^2\Delta_{3/2}, v^+=1, J^+)$ from the rotational levels, (a) $J'=2$, (b) $J'=3$, (c) $J'=4$, and (d) $J'=5$, of the intermediate $\text{VN}^*(D^3\Pi_0, v'=0)$ state.

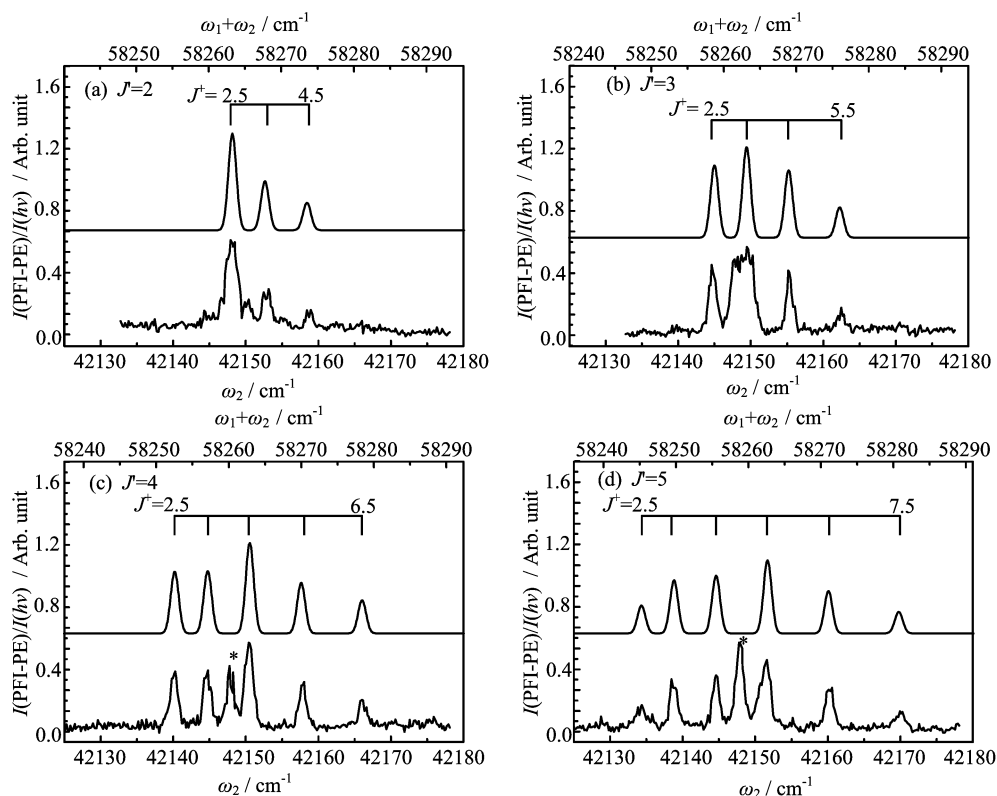


FIG. 7 Rotationally resolved PFI-PE spectra (lower) and the simulated spectra (upper) for the formation of $\text{VN}^+(X^2\Delta_{5/2}, v^+=1, J^+)$ from the rotational levels, (a) $J'=2$, (b) $J'=3$, (c) $J'=4$, and (d) $J'=5$, of the intermediate $\text{VN}^*(D^3\Pi_0, v'=0)$ state.

PFI-PE peaks, which are marked on top of the simulated spectra. The observation that the lowest allowed value of J^+ is $5/2$ confirms the symmetry of this state to be $^2\Delta_{5/2}$. The least-square fits give the rotational constant $B_0^+=0.6535\pm 0.0016\text{ cm}^{-1}$ and the band origin $\nu_{00}^+=57216.4\pm 0.8\text{ cm}^{-1}$ for the $\text{VN}^+(X^2\Delta_{5/2}, v^+=0)$ state.

We have also obtained the PFI-PE spectra for the formation of $\text{VN}^+(X^2\Delta_{3/2}, v^+=1, J^+)$ (lower spectra in Fig.6) and for the formation of $\text{VN}^+(X^2\Delta_{5/2}, v^+=1, J^+)$ (lower spectra in Fig.7) by employing the same procedures as described above. The upper spectra are the simulated spectra obtained by assuming a Gaussian instrumental line profile (FWHM of 1.8 cm^{-1}). The analysis of the spectra gives the rotational constant $B_1^+=0.6458\pm 0.0010\text{ cm}^{-1}$ and band origin $\nu_{10}^+=57965.6\pm 0.8\text{ cm}^{-1}$ for $\text{VN}^+(X^2\Delta_{3/2}, v^+=1)$ state and the rotational constant $B_1^+=0.6450\pm 0.0023\text{ cm}^{-1}$ and band origin $\nu_{10}^+=58272.2\pm 0.8\text{ cm}^{-1}$ for the $\text{VN}^+(X^2\Delta_{5/2}, v^+=1)$ state.

When the scan range was extended to the higher energies, the intensity of the PFI-PE signal was found to decrease drastically. We have only been able to record the PFI-PE spectra for the formation of $\text{VN}^+(X^2\Delta_{3/2}, v^+=2, J^+)$, which are depicted as the

lower spectra in Fig.8. On the basis of the least-square fits according to the standard formula, the rotational constant $B_2^+=0.6393\pm 0.0021\text{ cm}^{-1}$ and band origin $\nu_{20}^+=59010.6\pm 0.8\text{ cm}^{-1}$ for $\text{VN}^+(X^2\Delta_{3/2}, v^+=2)$ state can be determined.

In our previous PFI-PE study of the TiO/TiO^+ system, we found that many of the rotational structures observed in the VIS-UV PFI-PE spectra are strongly perturbed and the most intense transition from a given J' level is not always the transition with $|\Delta J^+|=|J^+-J'|=0.5$, *i.e.*, the transition corresponding to the smallest change in core rotational angular momentum. This result of the TiO/TiO^+ system is different from those obtained from previous state-to-state photoionization studies of the $\text{CH}_3\text{I}/\text{CH}_3\text{I}^+$, $\text{CH}_3\text{Br}/\text{CH}_3\text{Br}^+$, FeC/FeC^+ , NiC/NiC^+ , and CoC/CoC^+ systems, in which the change in core rotational angular momentum $|\Delta J^+|$ was found to have a value up to 5.5 and favor the smallest value, *i.e.*, photoionization cross section drops off as $|\Delta J^+|$ is increased [8, 10, 11, 15–17]. As shown in Figs. 4–8, the state-to-state PFI-PE spectra for the VN/VN^+ system reveal that the transition with $|\Delta J^+|=0.5$ always carries the highest transition intensity and the transition intensity decreases as $|\Delta J^+|$ is increased. Furthermore, only minor perturbations are observed in the re-

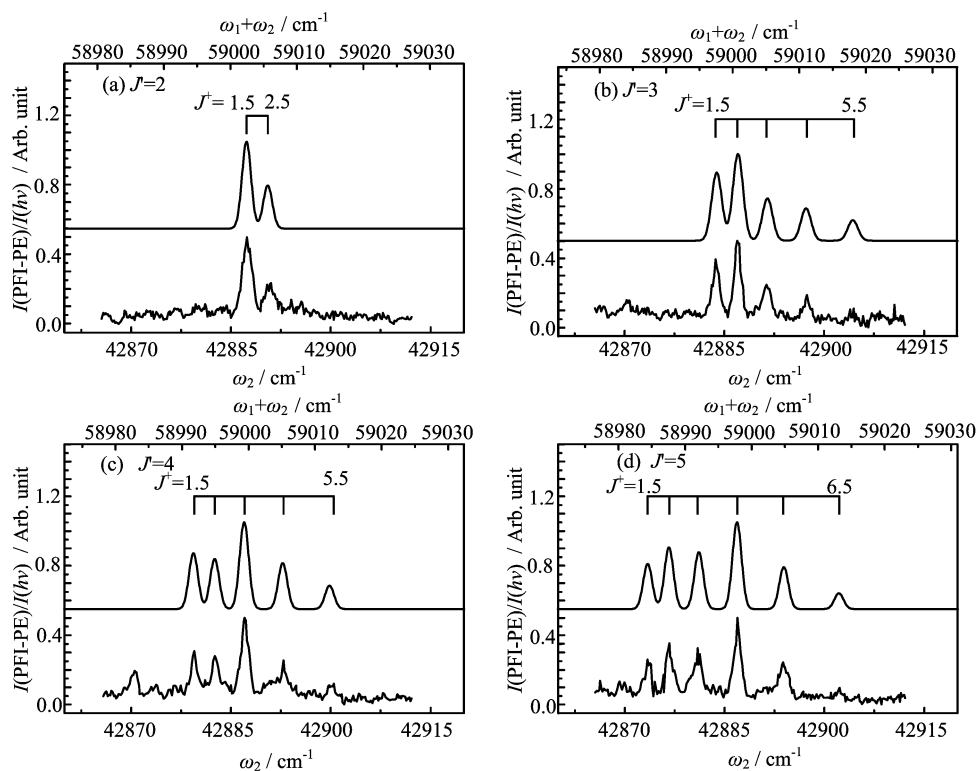


FIG. 8 Rotationally resolved PFI-PE spectra (lower) and the simulated spectra (upper) for the formation of $\text{VN}^+(X^2\Delta_{3/2}, v^+=2, J^+)$ from the rotational levels, (a) $J'=2$, (b) $J'=3$, (c) $J'=4$, and (d) $J'=5$, of the intermediate $\text{VN}^*(D^3\Pi_0, v'=0)$ state.

solved rotational structures of the PFI-PE spectra for VN/VN^+ . These findings are consistent with the results of the $\text{CH}_3\text{I}/\text{CH}_3\text{I}^+$, $\text{CH}_3\text{Br}/\text{CH}_3\text{Br}^+$, FeC/FeC^+ , NiC/NiC^+ , and CoC/CoC^+ systems; but differ somewhat compared to that observed in the TiO/TiO^+ system. Since TiO/TiO^+ and VN/VN^+ are isoelectronic and the neutral and cationic ground states have the same symmetry, the inconsistency is observed on the rotational photoionization. As Linton *et al.* pointed out in their study of YO^+ , the rotational photoionization could be governed by a channel-coupling mechanism [18]. The driving force of this mechanism is expected to be the dipole moment of MO species. The oxide of early transition metal elements, such as TiO and VN , are known to have strong ionic characters. Due to the higher electronegativity of O compared to N atom, the dipole moment of TiO is likely greater than that of VN . Thus, the stronger perturbation of rotational structures by near resonance interloper rotational Rydberg states observed in the TiO/TiO^+ photoionization system can be attributed by the greater dipole of TiO compared to that of VN .

Considering that the $\text{IE}(\text{VN})$ is defined to be the energy separation between the $\text{VN}^+(X^2\Delta_{3/2}, v^+=0, J^+=1.5)$ and $\text{VN}(X^3\Delta_1, v''=0, J''=1)$ states, we have determined the $\text{IE}(\text{VN})=56909.5\pm 0.8 \text{ cm}^{-1}$ ($7.05588\pm 0.00010 \text{ eV}$). This IE value is significantly

more accurate than the previously estimated value of $8\pm 1 \text{ eV}$ [7]. The $\text{IE}(\text{V})$ has been determined previously to be 6.7463 eV by Page *et al.* [19]. The accurate $\text{IE}(\text{VN})$ measurement also allows the determination of the $D_0(\text{V}^+-\text{N})-D_0(\text{V}-\text{N})=-0.3095 \text{ eV}$ by the IE difference, $\text{IE}(\text{V})-\text{IE}(\text{VN})$, based on the conservation of energy. The $D_0(\text{V}^+-\text{N})-D_0(\text{V}-\text{N})=-0.3095 \text{ eV}$ is compared to the $D_0(\text{Ti}^+-\text{O})-D_0(\text{Ti}-\text{O})=0.0084 \text{ eV}$. Similar to TiO , the electronic configuration of $\text{VN}(X^3\Delta_1)$ ground state is $\dots 7\sigma^2 8\sigma^2 9\sigma^1 3\pi^4 1\delta^1$ and the electronic configuration of $\text{VN}^+(X^2\Delta_{3/2})$ ground state is $\dots 7\sigma^2 8\sigma^2 3\pi^4 1\delta^1$. Thus to ionize VN in ground $X^3\Delta_1$ state requires removing the electron occupying the 9σ molecular orbital. The measured difference between $D_0(\text{V}^+-\text{N})$ and $D_0(\text{V}-\text{N})$ indicates the 9σ molecular orbital of neutral VN has relatively more bonding property compared to that of neutral TiO .

The electronic energy of a multiplet term can be written as:

$$T_e = T_0 + A\Lambda\Sigma \quad (5)$$

where T_0 is the electronic energy of the term when the spin-orbit coupling is neglected, A is spin-orbit coupling constant. According to the formula, the energy difference between $T_e(X^2\Delta_{5/2})$ and $T_e(X^2\Delta_{3/2})$ is equal to $2A$. Thus the spin-orbit coupling constant is determined to be $A=153.3\pm 0.8 \text{ cm}^{-1}$ for $\text{VN}^+(X^2\Delta_{5/2,3/2})$.

TABLE I Energetic and spectroscopic data obtained in the PFI-PE study, including ionization energies (IEs) for the formation of $\text{VN}^+(X^2\Delta_{3/2}, v^+=0-2)$ and $\text{VN}^+(X^2\Delta_{5/2}, v^+=0-1)$, rotational constants (B_0^+ , B_1^+ , B_2^+ , B_e^+ , and α_e^+), equilibrium bond distance (r_e^+), and vibrational constants ($\Delta G(1/2)$, $\Delta G(3/2)$, ω_e^+ , and $\omega_e^+\chi_e^+$) for $\text{VN}^+(X^2\Delta_{3/2}, v^+=0-2)$ and $\text{VN}^+(X^2\Delta_{5/2}, v^+=0-1)$, spin-orbit coupling constant A for $\text{VN}^+(X^2\Delta_{5/2,3/2})$ and the difference of D_0 values [$D_0(\text{V}^+-\text{N})-D_0(\text{V}-\text{N})$] for $\text{VN}^+(X^2\Delta_{3/2})$ and $\text{VN}(X^3\Delta_1)$.

	Parameter	$\text{VN}^+(X^2\Delta_{3/2}, V^+)^a$	$\text{VN}^+(X^2\Delta_{5/2}, v^+)^a$
$v^+=0$	v_{00}^+/cm^{-1}	56909.1±0.8	57216.4±0.8
	IE/ cm^{-1}	56909.5±0.8 ^b	57217.4±0.8 ^b
$v^+=1$	B_0^+/cm^{-1}	60000±8000 [7]	
	v_{10}^+/cm^{-1}	0.6530±0.0020	0.6535±0.0016
	IE/ cm^{-1}	57965.6±0.8	58272.2±0.8
	B_1^+/cm^{-1}	57965.9±0.8	58273.2±0.8
$v^+=2$	v_{20}^+/cm^{-1}	0.6458±0.0010	0.6450±0.0023
	IE/ cm^{-1}	59010.6±0.8	
	B_2^+/cm^{-1}	59010.9±0.8	
Rotational constant	B_e^+/cm^{-1}	0.6393±0.0021	
	$\alpha_e^+/\text{cm}^{-1}$	0.6563±0.0005	0.6578±0.0028
	$r_e^+/\text{Å}$	0.0069±0.0004	0.0085±0.0028
		1.529	1.527
Vibrational constant	$\Delta G(1/2)/\text{cm}^{-1}$	1056.5±0.8	1055.8±0.8
	$\Delta G(3/2)/\text{cm}^{-1}$	1045.0±0.8	
	$\omega_e^+/\text{cm}^{-1}$	1068.0±0.8	
	$\omega_e^+\chi_e^+/\text{cm}^{-1}$	5.8±0.8	
	A/cm^{-1}		153.3±0.8
	$[D_0(\text{V}^+-\text{N})-D_0(\text{V}-\text{N})]/\text{eV}$		-0.3095

^a This work.

^b The IE values give the spin-orbit coupling constant $A=153.3\pm 0.8 \text{ cm}^{-1}$ for $\text{VN}^+(X^2\Delta_{5/2,3/2})$.

The energy difference between two adjacent vibrational states is defined to be

$$\Delta G\left(v^+ + \frac{1}{2}\right) = G(v^+ + 1) - G(v^+) \quad (6)$$

$$G(v^+) = \omega_e^+ \left(v^+ + \frac{1}{2}\right) - \omega_e^+\chi_e^+ \left(v^+ + \frac{1}{2}\right)^2 \quad (7)$$

Based on the measured values of v_{00}^+ , v_{10}^+ , v_{20}^+ for $\text{VN}^+(X^2\Delta_{3/2})$ and v_{00}^+ , v_{10}^+ for $\text{VN}^+(X^2\Delta_{5/2})$, we have obtained $\Delta G(1/2)=1056.5\pm 0.8 \text{ cm}^{-1}$ and $\Delta G(3/2)=1045.0\pm 0.8 \text{ cm}^{-1}$ for $\text{VN}^+(X^2\Delta_{3/2})$ state and $\Delta G(1/2)=1055.8\pm 0.8 \text{ cm}^{-1}$ for $\text{VN}^+(X^2\Delta_{5/2})$ state, which determines $\omega_e^+=1068.0\pm 0.8 \text{ cm}^{-1}$ and $\omega_e^+\chi_e^+=5.8\pm 0.8 \text{ cm}^{-1}$.

By fitting the experimental rotational constants B_0^+ , B_1^+ and B_2^+ to the standard formula,

$$B_v^+ = B_e^+ - \alpha_e^+ \left(v^+ + \frac{1}{2}\right) \quad (8)$$

we have obtained the rotational constants B_e^+ and α_e^+ with the values of $0.6563\pm 0.0005 \text{ cm}^{-1}$ and $0.0069\pm 0.0004 \text{ cm}^{-1}$ for $\text{VN}^+(X^2\Delta_{3/2})$ state, $0.6578\pm 0.0028 \text{ cm}^{-1}$ and $0.0085\pm 0.0028 \text{ cm}^{-1}$ for

$\text{VN}^+(X^2\Delta_{5/2})$ state. The B_e^+ values have thus enabled the determination of the equilibrium bond distance $r_e^+=1.529 \text{ Å}$ for $\text{VN}^+(X^2\Delta_{3/2})$ state and $r_e^+=1.527 \text{ Å}$ for $\text{VN}^+(X^2\Delta_{5/2})$ state. All spectroscopic constants determined in this work are listed in Table I. The comparison between the experimental results for the TiO/TiO⁺ and VN/VN⁺ systems and the theoretical predictions by CCSDTQ/CBS calculations will be presented in a separated article.

IV. CONCLUSION

We have conducted a two-color VIS-UV resonance-enhanced PIE and PFI-PE study on cold gaseous VN generated by using a laser ablation supersonically beam source. The simulation of the measured rotationally well resolved PFI-PE spectra confirms that the VN⁺ ground state is of $^2\Delta_{3/2}$ symmetry. The unambiguous rotational assignment and analysis on the PFI-PE spectra for the formation of the $\text{VN}^+(X^2\Delta_{3/2}, v^+=0-2, J^+)$ and $\text{VN}^+(X^2\Delta_{5/2}, v^+=0-1, J^+)$ states has also enabled the determination of highly precise values for the IE(VN), the difference in 0 K bond energies between the VN⁺ cation and the VN neutral, spin-orbit coupling

constant, and vibrational and rotational constants for $\text{VN}^+(X^2\Delta_{3/2}, v^+=0-2)$ and $\text{VN}^+(X^2\Delta_{5/2}, v^+=0-1)$. The energetic and spectroscopic data obtained in this study has served as a reliable benchmark for theoretical predictions obtained based on state-of-the-art *ab initio* quantum calculations at the CCSDTQ/CBS level.

V. ACKNOWLEDGMENTS

This work was supported by the NSF Chemical Structures, Dynamics, and Mechanisms Program (No.CHE 0910488).

- [1] J. F. Harrison, *Chem. Rev.* **100**, 679 (2000).
- [2] W. J. Balfour, A. J. Merer, H. Niki, B. Simard, and P. A. Hackett, *J. Chem. Phys.* **99**, 3288 (1993).
- [3] J. F. Harrison, *J. Phys. Chem.* **100**, 3513 (1996).
- [4] K. L. Kunze and J. F. Harrison, *J. Phys. Chem.* **93**, 2983 (1989).
- [5] S. L. Peter and T. M. Dunn, *J. Chem. Phys.* **90**, 5333 (1989).
- [6] B. Simard, C. Masoni, and P. A. Hackett, *J. Mol. Spectro.* **136**, 44 (1989).
- [7] M. Farber and R. Srivasta, *J. Chem. Soc. Faraday Trans. I* **69**, 390 (1973).
- [8] Y. C. Chang, C. S. Lam, B. Reed, K. C. Lau, H. T. Liou, and C. Y. Ng, *J. Phys. Chem. A* **113**, 4242 (2009).
- [9] H. Huang, Z. H. Luo, Y. C. Chang, K. C. Lau, and C. Y. Ng, *J. Chem. Phys.* **138**, 174309 (2013).
- [10] Y. C. Chang, X. Y. Shi, K. C. Lau, Q. Z. Yin, H. T. Liou, and C. Y. Ng, *J. Chem. Phys.* **133**, 54310 (2010).
- [11] H. Huang, Y. C. Chang, Z. H. Luo, X. Y. Shi, K. C. Lau, and C. Y. Ng, *J. Chem. Phys.* **138**, 094301 (2013).
- [12] K. C. Lau, Y. C. Chang, C. S. Lam, and C. Y. Ng, *J. Phys. Chem. A* **113**, 14321 (2009).
- [13] K. C. Lau, Y. C. Chang, X. Y. Shi, and C. Y. Ng, *J. Chem. Phys.* **133**, 114303 (2010).
- [14] K. C. Lau, Y. Pan, C. S. Lam, H. Huang, Y. C. Chang, Z. H. Luo, X. Y. Shi, and C. Y. Ng, *J. Chem. Phys.* **138**, 094302 (2013).
- [15] P. Wang, X. Xing, K. C. Lau, H. K. Woo, and C. Y. Ng, *J. Chem. Phys.* **121**, 7049 (2004).
- [16] X. Xing, B. Reed, M. K. Bahng, S. J. Baek, P. Wang, and C. Y. Ng, *J. Chem. Phys.* **128**, 104306 (2008).
- [17] X. Xing, P. Wang, B. Reed, S. J. Baek, and C. Y. Ng, *J. Phys. Chem. A* **112**, 9277 (2008).
- [18] C. Linton, B. Simard, H. P. Loock, S. Wallin, G. K. Rothschof, R. F. Gunion, M. D. Morse, and P. B. Armentrout, *J. Chem. Phys.* **111**, 5017 (1999).
- [19] R. H. Page and C. S. Gudeman, *J. Opt. Soc. Am. B* **7**, 1761 (1990).